Power Consumption Analysis of Hybrid EDFA/Raman Amplifiers in Long-Haul Transmission Systems

Lars Lundberg, Peter A. Andrekson, *Fellow, IEEE, Fellow, OSA*, and Magnus Karlsson, *Senior Member, IEEE, Fellow, OSA*

***Abstract*—We analyze the power consumption of optical amplifiers and the tradeoff between power consumption and system performance. The power consumption model includes erbium-doped fiber amplifiers (EDFA), backwards pumped Raman amplification, and monitoring and management electronics. Performance is studied using the Gaussian-noise model for nonlinear interference. We find that the power consumption of the monitoring and management electronics has a large impact on system configuration that gives the lowest overall power consumption, where a low value favors shorter spans and EDFA-only amplification, while a high value favors longer spans with Raman amplification. Long total system lengths and high requirements on the optical signal-to-noise ratio also favors Raman amplification. Furthermore, we compare the amplifier energy consumption per bit for polarization-multiplexed quadrature phase-shift-keying and 16-quadrature amplitude modulation (16QAM). Our results show that 16QAM has a lower energy consumption per bit due to its higher spectral efficiency. We also find that it may be more energy efficient to increase the signal quality by shortening the spans or using Raman amplification than using powerful forward error correction with high power consumption.**

***Index Terms*—Optical amplifiers, optical fiber amplifiers, optical modulation, optical fiber communication, power consumption, energy efficiency.**

I. Introduction

OPTICAL amplification has since the introduction of the erbium-doped fiber amplifier (EDFA) been an indispensable part of long-haul fiber optical communication systems. The optical amplifiers also constitute a major part of the power consumption of an optical link. In the end-to-end power consumption analysis in [1], it was estimated that the EDFAs are responsible for 18% of the power consumption of a 2400 km system with 80×100 Gbit/s polarization-multiplexed quadrature phase-shift-keying (PM-QPSK) channels. In addition, the power consumption of the line amplifiers is a limiting factor for long-haul submarine cables [2], [3], since material properties limits the electrical power available in the cable.

Optical amplifiers are also responsible for one of the main sources of signal degradation, amplified spontaneous emission (ASE) noise. As described in [4] and further developed in [5], there is a tradeoff between the amplifier power consumption and the signal-to-noise ratio (SNR). This is due to the fact that the output signal power from an EDFA, which in the linear regime is directly related to the SNR, is proportional to the EDFA pump power [6]. However, the aforementioned investigations studied only the minimum bound, which is less useful for predicting the realistic power consumption and its connection to the signal quality, mainly for two reasons. The first reason is that fiber nonlinearities complicates the relation between the signal power and the signal quality. This issue was addressed in [7], where the Gaussian noise (GN) model for nonlinear interference (NLI) [8] was used as a starting point to derive two minimum energy consumption points; one corresponding to the optimum energy per bit and one corresponding to the optimum signal power for highest spectral efficiency. The second reason is that in currently available amplifiers, the power consumption is dominated by the monitoring and management electronics [4], [9], which can be expected to be independent of, e.g., signal output power and gain. Since the SNR also depends on the number of amplifiers, the inclusion of the monitoring and management power consumption significantly alters the relation between signal quality and power consumption.

Furthermore, while EDFAs is the most commonly used amplification technology, distributed Raman amplification offers lower ASE noise levels and potentially wider bandwidths than EDFAs [10]. Raman amplification is also inherently less energy efficient than EDFAs, which indicates that the improved noise performance or bandwidth comes at a cost in terms of power consumption. The performance benefits of Raman amplification are well known, also when the GN-model is used; in [11] the GN-model is extended to include Raman amplification and in [12] and [13] the performance benefits are analyzed. However, the implications of Raman amplification on the system power consumption has received little attention. In [14], we found that Raman amplification in some cases actually is capable of reducing the overall system power consumption by lessening the

Manuscript received September 16, 2016; revised November 16, 2016 and January 12, 2017; accepted February 9, 2017. Date of publication February 12, 2017; date of current version April 20, 2017. This work was supported by the Knut and Alice Wallenberg Foundation.

The authors are with the Department of Microtechnology and Nanoscience, Chalmers University of Technology, SE-412 96 Gothenburg, Sweden (e-mail: lars.lundberg@chalmers.se; peter.andrekson@chalmers.se; magnus.karlsson@chalmers.se).

Color versions of one or more of the figures in this paper are available online at http://ieeexplore.ieee.org.

Digital Object Identifier 10.1109/JLT.2017.2668768

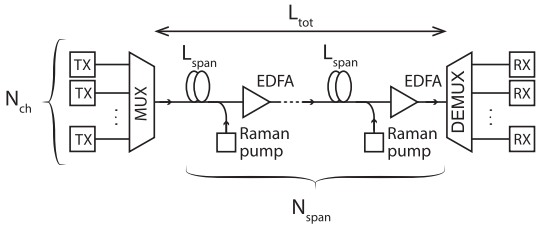

Fig. 1. Schematic of a long-haul transmission system of length L_{tot} with N_{ch} channels. Each span has a length of L_{span} and the span losses are compensated for with a combination of backwards pumped distributed Raman amplification and an EDFA.

burden on power hungry FEC circuits, a conclusion drawn also in [15].

In this paper we extend our work in [14] and develop a power consumption model for optical amplification that includes EDFAs and distributed Raman amplification, applicable to wavelength-division multiplexed (WDM) long-haul transmission systems. The aim is to give realistic estimates, so in addition to the pump laser power consumption also the power consumption of the monitoring and management electronics is accounted for. We investigate the connection between the power consumption and the system performance using the Gaussian noise model for NLI. In this way, a broad comparison of different system scenarios is made, including different amounts of Raman amplification, different span lengths and different system lengths. Furthermore, we compare PM-QPSK and PM-16QAM in terms of amplifier energy consumption per bit.

The remainder of this paper is organized as follows. In Section II, the system performance model is presented, and in Section III the power consumption model is described. Section IV investigates the tradeoff between power consumption and OSNR for single spans as well as multispan systems. In Section V, the relation between the energy consumption per bit and BER is analyzed. Section VI compares the results with those obtained in [15] and Section VII summarizes the paper.

II. System Performance Modeling

The analysis in this paper is based on a multispan link where the losses are compensated for by a combination of distributed Raman amplification and conventional EDFAs, illustrated in Fig. 1. In this section, the performance model used is presented. As is explained below we consider only backwards Raman pumping.

A. Raman Gain

In general, the signal power at the output of a Raman amplified span can be calculated by solving a set of coupled differential equations, which are not easy to solve analytically. However, if the pump power is assumed to be much larger than the signal power an analytical solution can be found. The Raman gain is conveniently expressed as the *on-off gain*, which is the ratio of the signal power at the output of the span with the pump turned on and the signal power at the output of the span with the pump turned off. In this paper, we will refer to this as simply the Raman gain. It can be written [10]

$$G_R = \exp\left(g_R P_R^p \frac{1-e^{-\alpha_p L}}{\alpha_p}\right) = \exp(g_R P_R^p L_{\text{eff}}), \quad (1)$$

where g_R is the Raman gain efficiency, P_R^p is the Raman pump power, $L_{\text{eff}} = (1-e^{-\alpha_p L})/\alpha_p$ is the pump effective length and α_p is the fiber loss coefficient at the pump wavelength. While this expression is valid for any combination of forwards and backwards pumping, the requirement that pump depletion should be negligible limits the applicability to backward pumping schemes.

For a general hybrid amplified span we can define the total gain as the product of the Raman gain G_R and the EDFA gain G_E, so that $G_{\text{tot}} = G_R G_E$. We then define the Raman gain ratio β_R as the ratio of the Raman gain to the total gain, most conveniently expressed in dB-scale, giving

$$G_{\text{R,dB}} = \beta_R G_{\text{tot,dB}}. \quad (2)$$

Here, we always assume that the total gain perfectly balances the fiber losses, so that $G_{\text{tot}} = e^{-\alpha_s L}$, where α_s is the fiber loss coefficient at the signal wavelength.

The Raman gain efficiency g_R depends on the fiber type, the pump frequency and the frequency difference between the pump and the signal. The gain resulting from a single pump does not cover the whole C-band, so for system applications multiple pumps need to be used. This further complicates the modeling since there will be a significant power transfer from the shorter wavelength pumps to the longer wavelength pumps. In general, a set of coupled equations need to be solved to analyze this situation. However, the total Raman gain still has an exponential dependence on the pump power [13], which means that Eq. (1) can still be used to find the power scaling if an appropriate scaling factor is used. To simplify modeling we calculate the needed pump power for the specified gain at 1550 nm and multiply with the number of Raman pumps. There are commercial Raman amplifier modules covering the C-band using two pumps [16], so we will assume that two pumps are enough to cover the C-band with sufficient gain flatness. We consider standard single mode fiber (SMF), which has a Raman gain efficiency of $g_R = 0.4\ \text{W}^{-1}\,\text{km}^{-1}$ [17].

B. Amplified Spontaneous Emission

Amplified spontaneous emission is the main signal impairment caused by both EDFAs and Raman amplification. The total ASE from a hybrid amplified span will be a sum of the ASE created in the EDFA and the Raman induced ASE, which also will be amplified in the EDFA, so that

$$S_{\text{ASE}} = S_{\text{ASE,E}} + G_E S_{\text{ASE,R}}. \quad (3)$$

The ASE from the EDFA can be found using the well known expression [6]

$$S_{\text{ASE,E}} = n_{\text{sp,E}} h\nu (G_E - 1), \quad (4)$$

while the Raman ASE requires integration over the whole span length [10],

$$S_{\text{ASE,R}} = n_{\text{sp,R}} h\nu g_R G_R e^{-\alpha_s L} \int_0^L \frac{P_R^p(z)}{\Gamma(z)} dz, \tag{5}$$

where $P_R^p(z)$ is the pump power at position z along the fiber, and $\Gamma(z) = P_s(z)/P_s(0)$ is the normalized signal power at position z along the fiber, also known as the signal power profile or net gain profile. Equation (5) is valid when pump depletion is negligible, and the Raman induced ASE is then independent of the input signal power. The expressions for the powers as a function of z can be found in [10, Ch. 2].

C. Nonlinear Interference

In modern coherent fiber optical communication systems where dispersion is compensated for using digital signal processing (DSP) and no optical dispersion compensation is used, the impact of nonlinearities on the signal can often be treated as Gaussian noise [8]. While there are relatively simple formulas for calculating the nonlinear noise PSD for passive spans, i.e. spans without distributed amplification, for a general Raman amplified span the signal power profile must be integrated over the span length [11]. However, for some specific cases the increase in nonlinear noise due to distributed amplification is negligibly small. In [12] numerical simulations is used to establish that for backwards pumping with the Raman gain ratio $\beta_R < 60\,\%$, this is the case. This also coincides with the regime where pump depletion is negligible [12]. We will limit our analysis to this region. Similarly, in [13] NLI is found to not make a significant difference for backwards pumped spans if the output power is at least 13 dB below the input power.

The fundamental of the GN-model is that the effect of nonlinearities can be described as additive white Gaussian noise, which leads to the effective OSNR

$$\text{OSNR} = \frac{P_s}{2N_{\text{span}}(S_{\text{ASE}} + S_{\text{NLI}})\Delta\nu}, \tag{6}$$

where the NLI spectral density S_{NLI} depends on the power, spectral shape and frequency spacing of all the WDM channels in the system [18]. In the case of identical channels with rectangular spectra, we can write

$$S_{\text{NLI}} = k_{\text{NLI}} \left(\frac{P_s}{2}\right)^3, \tag{7}$$

where k_{NLI} depends on the number of channels, the bandwidth and the channel spacing. It can be calculated with [18, Eq. (16)].

By inserting Eq. (7) into Eq. (6) and differentiating with respect to P_s an optimum signal power that maximizes the OSNR can be found. This signal power can be written

$$P_{\text{opt}}^s = 2\left(\frac{S_{\text{ASE}}}{2k_{\text{NLI}}}\right)^{1/3}. \tag{8}$$

From this it follows that the optimum signal power will depend on the level of ASE, which is affected by span length and amount of Raman amplification. It is important to realize that this will have implications on the amplifier power consumption.

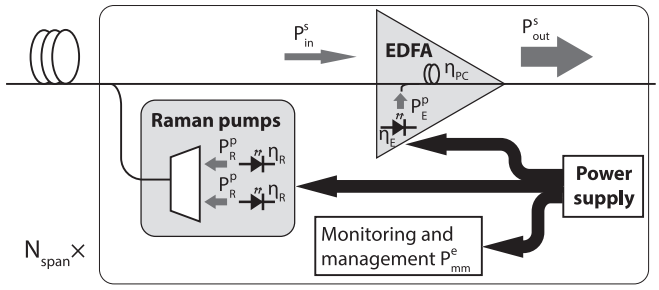

Fig. 2. Schematic of the amplifier power consumption model. The optical output power of each Raman pump laser is P_R^p and the EDFA pump power is P_E^p. The pump lasers has a electrical-to-optical power conversion efficiency of η_E and η_R respectively, and in the erbium-doped fiber the pump power is converted to signal power with an efficiency of η_{PC}. The signal power at the input and output of the EDFA is denoted P_{in}^s and P_{out}^s, respectively.

D. Other Raman Induced Signal Impairments

In addition to an increased nonlinear penalty, Raman amplification may induce other signal impairments, including multi-path interference caused by double Rayleigh scattering, polarization-dependent gain and pump-to-signal noise transfer. While these effects are important to consider when designing Raman amplified systems, in the moderate backwards pumped regime considered in this paper they can be neglected [13].

III. Power Consumption Model

A schematic of the power consumption model can be seen in Fig. 2. We follow the approach in [4], where the power consumption is divided into two main parts. The first part is the power consumption related to the key function, which in our case is the power consumption of the EDFA and Raman pump lasers. The second part is a fixed power consumption to account for various functions not related directly to the key function, which we will refer to as the monitoring and management power consumption. The power consumption of the pump lasers is directly proportional to the optical output power of the laser [4]. We note that in [5] and [15], a constant term was added to the pump laser power consumption to account for the power consumption at the laser threshold. We consider this constant term to be included in the monitoring and management power consumption. The total power consumption for one span is thus

$$P_{\text{span}}^e = \frac{1}{\eta_E} P_E^p + \frac{N_R}{\eta_R} P_R^p + P_{\text{mm}}^e, \tag{9}$$

where P_E^p and P_R^p are the EDFA and Raman optical pump powers respectively, η_E and η_R are the respective electrical to optical power conversion efficiencies, N_R accounts for the number of Raman pumps needed to cover the wavelength range considered and P_{mm}^e is the monitoring and management power consumption.

In general, both the Raman and EDFA pump powers are functions of the total signal power, the gain, and the amount of ASE added to the signal. However, for the system scenarios considered in this work, the Raman amplification is operated in the moderate pumping regime where pump depletion is negligible [12], Then, the Raman pump power is only dependent on the

distributed gain and the span length [10]. This means that the Raman pump power can be determined directly from Eq. (1).

For an EDFA, the absolute minimum pump power needed is [6]

$$P_E^p = \frac{\lambda_s}{\lambda_p}(P_{\text{out}}^s - P_{\text{in}}^s), \tag{10}$$

which states that the pump power is proportional to the power added to the signal, with a power conversion factor λ_s/λ_p corresponding to the energy difference between the pump and signal wavelengths. This equation follows from photon number conservation and represents an ideal situation where all of the pump photons are converted into signal photons. Nevertheless, as we show in Appendix A, this equation still describes the pump power well in the operating regime we consider if the ideal power conversion factor is replaced with a non ideal power conversion efficiency $1/\eta_{\text{PC}} > \lambda_s/\lambda_p$.

The important conditions is that the total output signal power is large and that the EDF length is optimised for the specific output power and gain. The first condition is typically fulfilled for a WDM-system with all channels in use, and the second means that this analysis is applicable not to a specific EDFA operating at the different conditions but rather assuming that the EDFA is optimised for the specific system scenario.

The signal power at the input of the EDFA can be written in terms of the EDFA gain and the output power $P_{\text{in}}^s = P_{\text{out}}^s/G_E = N_{\text{ch}}P_{\text{ch}}^s/G_E$, where P_{ch}^s is the signal power per channel. Now, we arrive at the final expression for the EDFA pump power,

$$P_E^p = \frac{1}{\eta_{\text{PC}}}N_{\text{ch}}P_{\text{ch}}^s\left(1 - \frac{1}{G_E}\right). \tag{11}$$

Inserting this expression and Eq. (1) into Eq. (9) and multiplying with the number of spans we arrive at

$$P_{\text{tot}}^e = N_{\text{span}}\left(\frac{1}{\eta_{\text{EPC}}}N_{\text{ch}}P_{\text{ch}}^s\left(1 - \frac{1}{G_E}\right) + \frac{N_R}{\eta_{\text{R}}}\ln\frac{G_R}{g_R L_{\text{eff}}} + P_{\text{mm}}^e\right). \tag{12}$$

Here, $\eta_{\text{EPC}} = \eta_E\eta_{\text{PC}}$ is the overall power conversion efficiency of the EDFA, from electrical power to power added to the signal. The energy consumption per bit can be found by dividing this expression with the total bitrate of the whole system,

$$E_{\text{bit}} = \frac{P_{\text{tot}}^e}{N_{\text{ch}}R_b} = \frac{P_{\text{tot}}^e}{2N_{\text{ch}}kR_s}, \tag{13}$$

where k is the number of bits per symbol per polarization in the modulation format used and R_s is the symbol rate. We assume a fixed symbol rate which is equal to the channel bandwidth $R_s = \Delta f$.

The power conversion efficiencies used above account for many different sources of inefficiencies. In the Raman case, it includes the power conversion of the laser diode and coupling losses in monitoring taps. In addition, as Raman pump lasers need to be temperature controlled, the power consumption of the thermoelectric cooler (TEC) is also included. The efficiency of the laser diode can reach 25% [19], but the power consumption of the TEC significantly contributes to the power consumption and lowers the overall efficiency. In Appendix B we describe how the TEC power consumption can be modelled. We use a TEC coefficient of performance of 17% typical for a 50 K temperature difference [20], which corresponds to a worst case scenario where the ambient temperature is 75 °C and the laser is kept at 25 °C. Combining these inefficiencies with 1.5 dB coupling losses we assume an overall power conversion efficiency of $\eta_R = 3\%$. In the EDFA case, the conversion efficiency includes power conversion in the pump laser, pump to signal power conversion in the EDF and losses in gain-flattening filters. As in [3] we assume an overall power conversion efficiency of $\eta_{\text{EPC}} = 5\%$, which assumes that the EDFA pump laser can be used without cooling. As a reference, the power consumption of an EDFA pump laser amplifying a WDM system with a total output signal power of 20 dBm with 20 dB gain is 2 W.

TABLE I
SYSTEM PARAMETERS

Symbol	Quantity	Value
N_R	Raman pump multiplicity	2
η_R	E/O conversion efficiency of Raman pump laser	3%
η_{EPC}	EDFA power conversion efficiency, including E/O conversion efficiency of pump laser	5%
N_{ch}	Number of channels	80
f_{space}	Channel spacing	50 GHz
Δf	Channel bandwidth	28 GHz
$\Delta\nu$	OSNR reference bandwidth	12.5 GHz
λ_s	Signal wavelength	1550 nm
λ_p	Raman pump wavelength	1450 nm
α_s	Fiber attenuation at λ_s	0.2 dB/km
α_p	Fiber attenuation at λ_p	0.25 dB/km
$n_{\text{sp,E}}$	Spontaneous emission factor for EDFA	1.58
$n_{\text{sp,R}}$	Spontaneous emission factor for Raman	1.13
g_R	Raman gain efficiency	0.4 W^{-1} km^{-1}
D	Dispersion parameter	16 ps nm^{-1} km^{-1}
γ	Nonlinear parameter	1.3 W^{-1} km^{-1}

The fiber parameters correspond to a standard SMF.

The choice of the value of the monitoring and management power consumption deserves some discussion. In [4] it was stated that the total power consumption of an EDFA is 100 W, and in [1] a monitoring and management power consumption of 55 W was used. Van Heddeghem *et al.* [21] have based their estimates on a generalization of data sheet values and use values between 30 W and 60 W total amplifier power consumption depending on span length. However, in [3] a value of 10 % of the total amplifier power consumption was used, which would correspond to only 0.2 W for the system mentioned above. In most of the analysis in this paper we use a value of 10 W, but due to the uncertainty in the estimate we investigate the effect of other values as well in several cases. The rest of the system parameters used are listed in Table I. The fiber parameters correspond to a standard SMF with 80 μm^2 effective area.

IV. POWER CONSUMPTION AND PERFORMANCE OF HYBRID AMPLIFIED SYSTEMS

A. Single Span

We start by studying a single hybrid amplified span where the losses are fully compensated for by a combination of

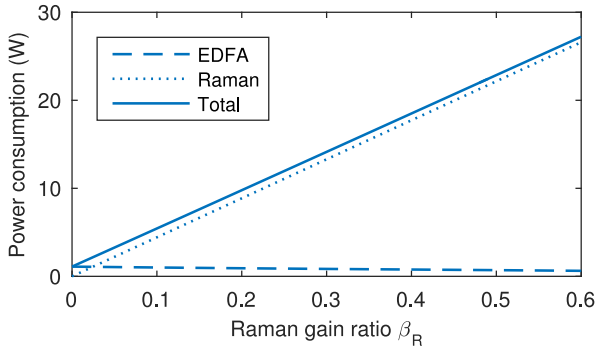

Fig. 3. Total pump power consumption as a function of Raman gain ratio for a 100 km span. The power consumption includes inefficiencies and in the Raman case a factor of two accounting for the need to have several pumps to cover the C-band.

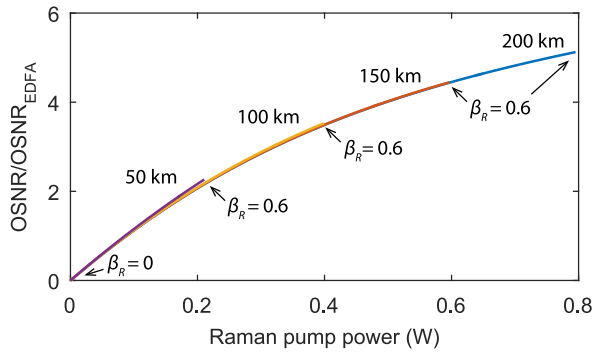

Fig. 4. Normalized OSNR-increase as a function of Raman pump power, where the Raman gain ratio is swept from $\beta_R = 0$ to $\beta_R = 0.6$. The different colors correspond to different span lengths. Note that the same Raman gain ratio corresponds to different pump power levels for different span lengths.

Raman amplification an EDFA. By studying how the pump laser power consumption and ASE noise power is changed when the amount of Raman amplification is changed we can gain insight into the tradeoffs involved. As noted earlier in Eq. (1) the Raman pump power depends linearly on the Raman gain in dB, from which it follows that it depends linearly also on the Raman gain ratio β_R. The EDFA pump power, described in Eq. (11), has only a weak dependence on the gain but depends linearly on the signal power at the output of the amplifier. Due to the weak gain dependence of the pump power, if the EDFA output signal power is kept unchanged when the Raman gain is increased, the EDFA power consumption will be approximately unchanged. However, if NLI is taken into account and the system is operated at the optimal signal power, the signal power depends on the ASE power according to Eq. (8). This means that the EDFA pump power can be decreased when Raman amplification is used. While this power consumption decrease is not insignificant, it is shadowed by the addition of the Raman pump power consumption, which can be seen in Fig. 3 where the EDFA and Raman pump power consumption is plotted as a function of the Raman gain ratio for a 100 km span.

While the added Raman pump leads to a higher power consumption, this is associated by a decrease of the noise power. The noise reduction normalized to the noise level for an equivalent EDFA amplified span does not depend much on the span length as seen in Fig. 4, since the Raman amplification takes place mostly in the end of the fiber. This means that the OSNR improvement only depends on the Raman pump power. However, the reduction of ASE does not fully describe the OSNR improvement if NLI is also included. As discussed earlier, a reduction of the ASE will also lead to a reduction of the optimal signal power. In fact, at the optimal signal power, the OSNR is inversely proportional to $S_{\mathrm{ASE}}^{2/3}$, which leads to the OSNR improvement in dB being only $2/3$ of the ASE reduction. This was previously noted in [22].

B. Multispan

The insensitivity of the OSNR improvement to the span length makes it easy to do quick estimations of the power consumption change associated with an increased OSNR also in multispan systems with identical spans, provided that the number of spans is kept constant. If the same amount of Raman pump is injected to each of the spans, the OSNR increase is the same as that for a single span, and the increase in power consumption can be found by simply multiplying the number of spans with the Raman pump power consumption. An example of such a comparison can be found in our previous work [14].

However, in multispan systems the OSNR is also affected by the span length (or the number of spans), which adds another degree of freedom in the system design. As is well known, using shorter span lengths is an effective way of increasing the OSNR. The ASE decrease then leads to a decrease in optimal signal power and consequently a decrease in EDFA pump power consumption for each amplifier unit. However, since the number of amplifier units then is increased, the relation between total pump power consumption and OSNR is not trivial. In fact, based on the GN-model it can be shown analytically that there is an optimum span length that minimizes the total pump power consumption at a specific OSNR-level [7]. When using a different number of spans also the power consumption of the monitoring and management circuits changes, since each amplifier unit consumes a fixed amount of power for this. The total monitoring and management power consumption hence depends linearly on the number of spans. As discussed earlier, the values for this power consumption found in the literature varies widely, and are in most cases estimated to be significant compared to the power consumption of the pump lasers. Considering this, a comparison between systems with different number of spans cannot be made without taking the monitoring and management power consumption into account.

In the following analysis we study the relation between the OSNR and the total power consumption by comparing system scenarios with the same total length, but different number of spans, and different amounts of Raman amplification. Changing the number of spans in an existing system is not trivial. Thus, this analysis applies to e.g. green field installations. It also highlights general-level tradeoffs involved when choosing span lengths and amplifier schemes.

In Fig. 5 a breakdown of the total power consumption for EDFA only and Raman assisted systems is plotted as a function

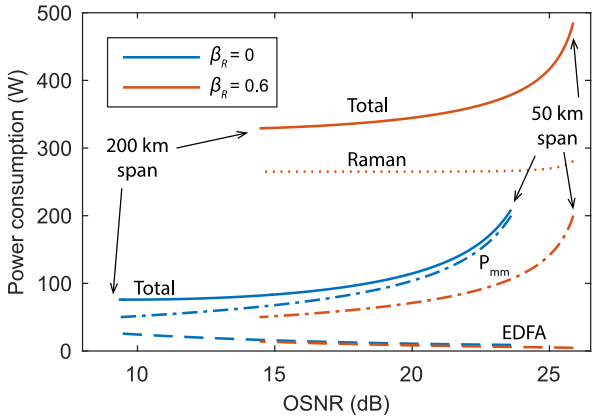

Fig. 5. Total power consumption of EDFA pumps (dashed lines), Raman pumps (dotted lines) and monitoring and management (dash-dotted lines) as a function of OSNR for systems with a total length of 1000 km and $P^e_{\text{mm}} = 10$ W. Two amplifier schemes are consider; one EDFA-only and one $\beta_R = 0.6$ hybrid Raman. The OSNR is varied by changing the number of spans between 5 and 20, which corresponds to span lengths of between 50 and 200 km. The end points of the curves correspond to this range.

of the OSNR. The total length is 1000 km and $P^e_{\text{mm}} = 10$ W. The OSNR is varied by changing the span length between 50 and 200 km. As discussed earlier, the EDFA pump power decreases with increasing OSNR, while the monitoring and management power consumption increase with increasing OSNR. This can give rise to a situation where a minimum power consumption is achieved when the increase of monitoring and management power consumption is balanced by the decrease of the pump power consumption.

The addition of the two Raman pumps to each span increases the OSNR, but also leads to a significant increase in the power consumption. Since the Raman amplification takes place mostly towards the end of the fiber, the total Raman pump power consumption is nearly constant regardless of span length, and only increases slightly when the span length approaches 50 km. Thus the Raman pump power needed can be considered to only depend on the Raman gain ratio and the total loss in the system for the span lengths considered here.

In this example, Raman amplification provides no benefit over only-EDFA in terms of power consumption, but this conclusion is highly dependent on the value assumed for the monitoring and management power consumption. This can be seen when comparing Fig. 6(a) and (b), where the total power consumption is plotted as a function of the OSNR for two values of the monitoring and management power consumption. In (a), with a larger monitoring and management power consumption, the lowest power consumption for OSNR values above 22 dB is achieved with Raman amplification, while in (b), which represents the same system as in Fig. 5 adding Raman amplification only increases the power consumption.

The optimum amount of Raman amplification can be found by studying different system scenarios with the same total length and the same OSNR but changing the amount of Raman amplification. Then, the number of spans differs between the different scenarios in order to keep the same OSNR. The minimum power consumption is a tradeoff between the monitoring and management power consumption and the Raman pump power consumption. Obviously, different values of the monitoring and management power consumption will give different optima, as will also different total lengths and OSNR-values. In Fig. 6(c) and (d) the power consumption as a function of the Raman gain ratio is plotted for two OSNR-values. Every line corresponds to a different monitoring and management power consumption. For the low values of P^e_{mm}, the minimum power consumption is achieved with no Raman amplification, but a higher value of P^e_{mm} shifts the optimum towards more Raman amplification. A higher OSNR requirement also favors more Raman amplification.

While these examples are for a 1000 km system, the general behaviour is the same regardless of system length. For example, a doubling of the system length while keeping the individual span lengths constant will double the number of spans and thus double the power consumption and lower the OSNR with 3 dB.

V. Energy Consumption per Bit, BER, and Modulation Formats

A. Comparison of Modulation Formats

The OSNR, together with the choice of modulation format governs the achievable BER, and the spectral efficiency of the modulation format determines the total data throughput of the system. This allows us find the energy per bit as a function of BER, and also compare different modulation formats.

First, we compare PM-QPSK and PM-16QAM at the same symbol rate. In this case, the bit-rate is doubled for 16QAM compared to QPSK, due to the doubled spectral efficiency. However, this comes at the cost of an increased OSNR requirement for 16QAM, which gives rise to a tradeoff situation between the energy consumption per bit and spectral efficiency.

Figure 7 shows the energy consumption per bit as a function of the BER for PM-QPSK and PM-16QAM for different system lengths. The BER was calculated using [23, Eqs. (4.3-31) and (4.3-32)], assuming Gray encoding and only nearest neighbor errors. To account for various system imperfections an OSNR penalty of 3 dB was subtracted before the BER was calculated. For shorter systems the BER can be decreased with a relatively small increase in energy consumption, while longer systems require a larger increase. Even if 16QAM requires a higher OSNR for the same BER, the doubled spectral efficiency leads to the energy per bit still being lower than for QPSK, except for the lowest BER values. In accordance with the results from the previous sections, there is no benefit of Raman amplification if the modulation format is not changed, as long as the monitoring and management power consumption is low. However, Raman amplification in combination with 16QAM can lead to a lower energy consumption per bit than QPSK and EDFA only amplification, for higher values of the monitoring and management power consumption. This can be seen in Fig. 7(d).

The dependence on the system length can be studied by calculating the number of spans needed to achieve a certain OSNR level for every system length, and then calculating the corresponding energy consumption per bit. The number of spans increases in a faster-than-linear fashion since, in addition to the

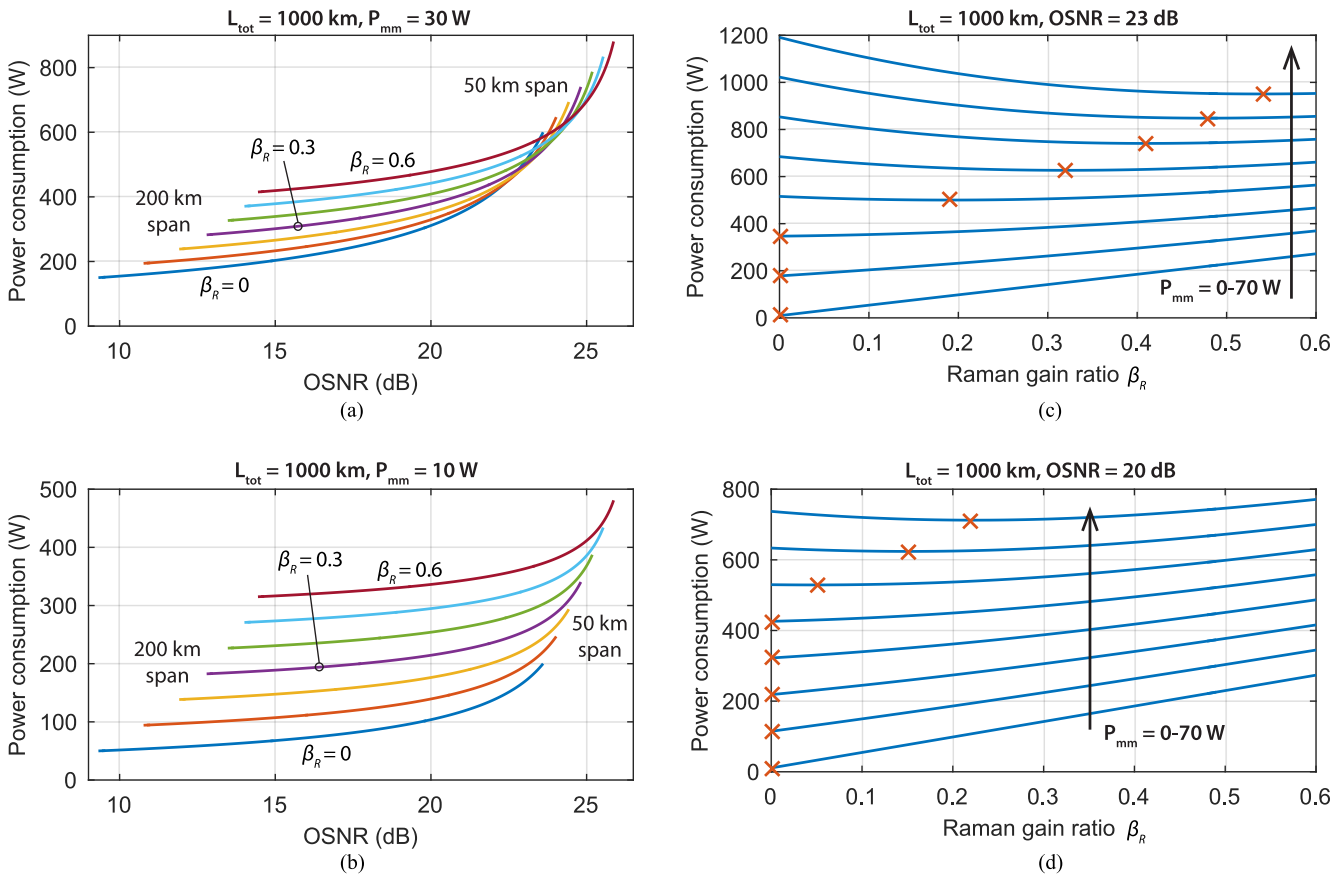

Fig. 6. (a) and (b) Power consumption as a function of OSNR. The different curves correspond to different Raman gain ratios. The OSNR is varied by changing the number of spans between 5 and 20, which corresponds to span lengths of between 50 and 200 km. The end points of the curves correspond to this range. (c) and (d) Power consumption as a function of Raman gain ratio for a fixed system length and OSNR. Each curve corresponds to a different value of P^e_{mm}. Red crosses mark the minimum power consumption.

linear increase needed to increase the system length, the required OSNR-level enforces the use of shorter spans to reduce the noise. Setting a minimum value for the span length then sets a limit for the reach of the system. Figure 8 shows the energy consumption per bit as a function of the system length for PM-QPSK and PM-16QAM at a BER of 10^{-2}. In this case, 16QAM and EDFA-only achieves the lowest energy consumption per bit for system lengths below 1800 km, above which QPSK and EDFA-only is the most energy-efficient. However, the difference is small between QPSK and 16QAM using only EDFA. Comparing 16QAM and QPSK using Raman amplification, 16QAM consistently has a lower energy consumption per bit. Due to the higher OSNR requirement, the reach of 16QAM is limited by the constraint of having spans longer than 50 km.

B. Energy Consumption per Bit Including FEC

Many coherent long-haul systems rely on the use of FEC to achieve acceptable BER values. The power consumption of the encoding and decoding circuits can be significant [1], and depends on among other things the error correcting capabilities of the code. A higher error correcting capability means that the system can be operated at a lower OSNR-level and a lower amplifier power consumption while the post-FEC BER is maintained. This essentially creates a tradeoff between amplifier and FEC power consumption. A full investigation of this tradeoff is outside the scope of this work since the relation between FEC power consumption and error correction capabilities is not straightforward to find. However, using the model for amplifier power consumption developed in this paper together with power consumption estimates from other work provides some insight. Based on [1], a hard decision Reed-Solomon code requiring a pre-FEC BER of 10^{-4} consumes in total for encoding and decoding $1.3\,\text{pJ/bit}$, while an LDPC code requiring a pre-FEC BER of 10^{-2} consumes as much as $130\,\text{pJ/bit}$.

In Fig. 9, the energy consumption per bit for QPSK is plotted for BER values of 10^{-4} and 10^{-2}, with the FEC energy consumption per bit corresponding to the BER values added. This shows that for system lengths below 3700 km, the Reed-Solomon scheme and EDFA-only amplification is the most energy efficient. Above 3700 km, Raman amplification is needed to keep the span length above 50 km, but the Reed-Solomon scheme is still more energy efficient until the system length reaches 5000 km, above which the lower OSNR requirements of the LDPC scheme results in a lower overall power consumption despite the power hungry FEC-circuits. Thus the EDFA-based solution is the most energy efficient, but limits the reach. If longer reach than 3700 km is needed, and the alternatives are the above two FEC-implementations, adding Raman amplification is more energy efficient than using a more powerful

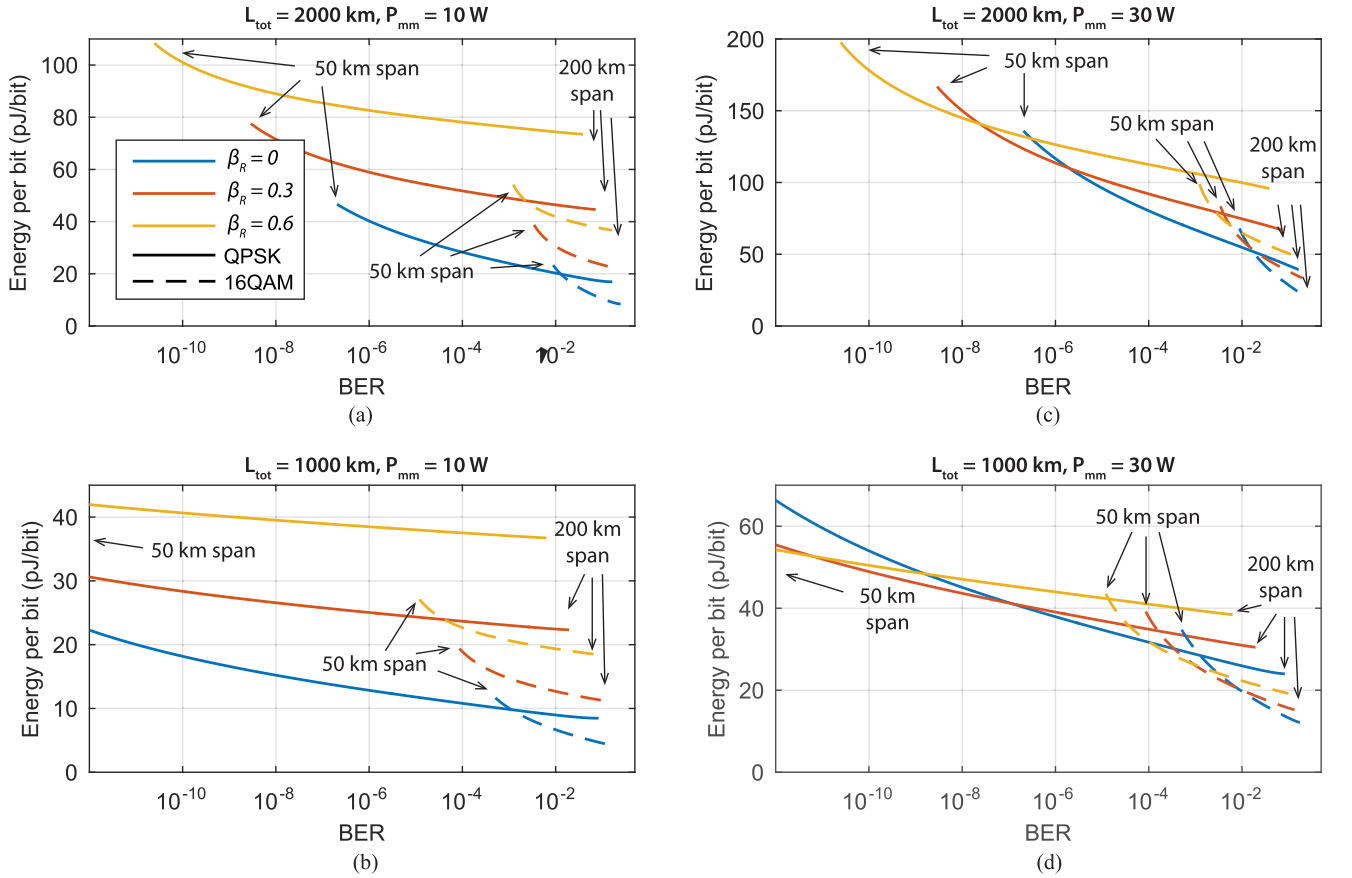

Fig. 7. Power consumption versus BER for different system lengths and values of P^e_{mm}. The OSNR is varied by changing the span length from 50 to 200 km. The end points of the curves correspond to this range.

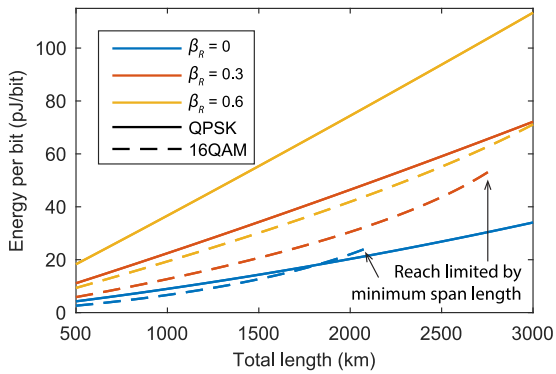

Fig. 8. Energy per bit versus L_{tot} at a constant OSNR, corresponding to a BER of 10^{-2} for PM-QPSK and PM-16QAM, with $P^e_{\text{mm}} = 10$ W. The span length is kept above 50 km which limits the maximum L_{tot}. The end points of the curves correspond to this condition.

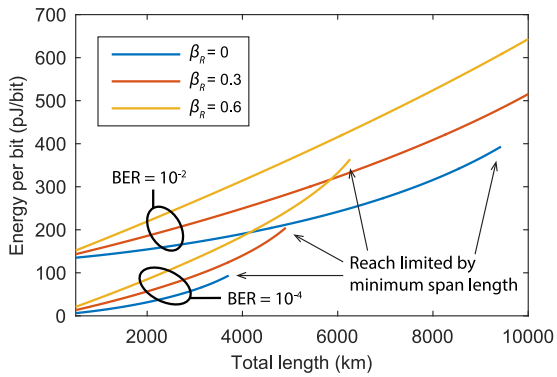

Fig. 9. Energy per bit versus L_{tot} for QPSK at a constant OSNR, including FEC power consumption. BER values are pre-FEC. Energy per bit values are scaled to account for a FEC overhead of 7% and 20% in the BER $= 10^{-4}$ and BER $= 10^{-2}$ cases respectively. $P^e_{\text{mm}} = 10$ W. The span length is kept above 50 km which limits the maximum L_{tot}. The end points of the curves correspond to this condition.

FEC. However, it should be stressed that the above results are highly dependent on the power consumption of FEC circuits, which can be expected to decrease in the future due to developments in CMOS technology and code design. For example, in [24] codes are presented with similar performance to the LDPC code used above but with an energy consumption below 3 pJ/bit.

In addition, comparisons between amplifier power consumption and transceiver power consumption might not always be fair, as they take place in different parts of the systems. For example, in submarine links power to the amplifiers is limited by the power available in the cable [2], [3].

C. At the Achievable Rate

By combining the OSNR found with the GN-model with the formula for the Shannon capacity, $C = \log_2(1 + \text{SNR})$, the

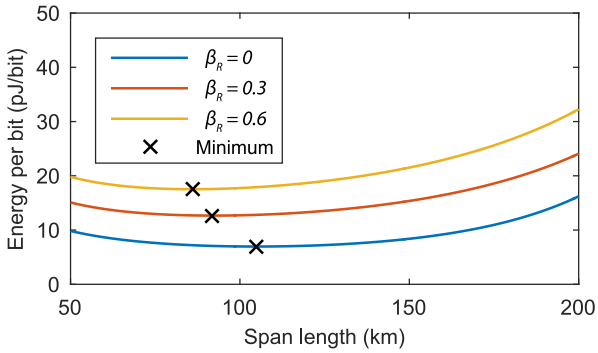

Fig. 10. Energy per bit as a function of span length assuming that every channel is operating at the achievable rate for $L_{\text{tot}} = 2000\,\text{km}$ and $P^e_{\text{mm}} = 10\,\text{W}$. Crosses mark minimum value.

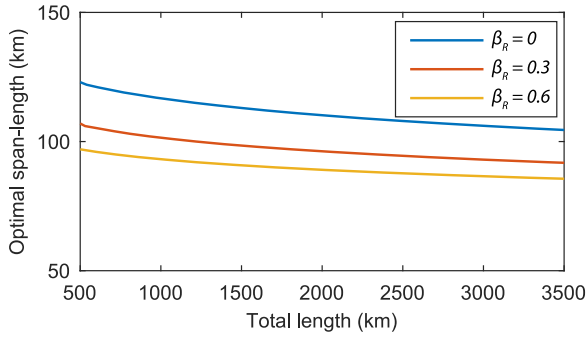

Fig. 11. Optimum span length corresponding to the minimum energy consumption per bit at the achievable rate as a function of the total length. $P^e_{\text{mm}} = 10\,\text{W}$

achievable rate of the system can be found. This is a lower bound [25] on the nonlinear fiber Shannon capacity (the actual capacity is unknown), under the restriction that the channel is well modeled by the GN model. This achievable rate was analyzed in [26] and also used in the power consumption analysis in [7].

In Fig. 10 the energy per bit assuming that every channel is operating at the achievable rate is plotted as a function of the span length for a total length of 2000 km. No margin is added to the OSNR and the channel bandwidth is taken to be the same as the channel spacing, 50 GHz. The total number of channels is 80, giving a total bandwidth of 4 THz. It reveals a clear tradeoff situation between a higher energy consumption for shorter span lengths and a lower capacity at longer span lengths, which causes a higher energy consumption per bit. Furthermore, as can be seen in Fig. 11, the optimal span length only decreases slowly with an increasing system length.

VI. Discussion

In [15] Wang *et al.* investigates the limits of attainable energy efficiency of EDFA and Raman amplified links. Here we compare their results to ours. Comparing just the amplifier power consumption, Wang *et al.* conclude that Raman amplification is always less energy efficient, which we also find if only the pump power consumption is considered. However, if in contrast to the analysis by Wang *et al.* the monitoring and management power consumption is considered, Raman amplification can be

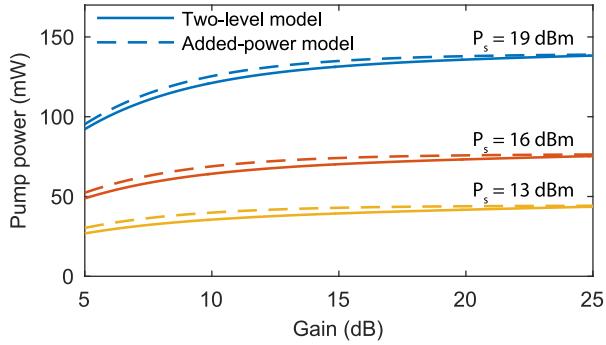

Fig. 12. Pump power calculated with the two-level model compared with pump power calculated with the added-power model. For the two-level model, the EDF length is optimized for highest energy conversion in each point, and the power conversion efficiencies for the added-power model are $\eta_{\text{E}} = 45\%$, $\eta_{\text{E}} = 52\%$ and $\eta_{\text{E}} = 57\%$ respectively for signal output powers of $P^s_{\text{out}} = 13\,\text{dBm}$, $P^s_{\text{out}} = 16\,\text{dBm}$ and $P^s_{\text{out}} = 19\,\text{dBm}$

more energy efficient. Furthermore, Wang *et al.* find that when 16QAM achieves an acceptable BER, it is always more energy efficient, while in our analysis we find that in some cases 16QAM can lead to a higher energy consumption per bit. The difference is again that Wang *et al.* does not consider monitoring and management power consumption in combination with not comparing the two modulation formats at the same BER. Finally, in agreement with our results, Wang *et al.* find that adding Raman amplification to increase the reach may be more energy efficient than using more powerful FEC in some cases when the choice of FEC implementations is limited.

VII. Conclusion

A power consumption model for optical amplifiers in long-haul fiber optical communication systems has been developed. The model includes both EDFA and distributed Raman amplification, and takes into account pump power consumption and management electronics. It is combined with the GN-model for nonlinear signal distortion to analyze the tradeoff between amplifier power consumption and signal quality at the nonlinear limit. We have used this model to analyze the both single spans and multispan systems.

We find that when power consumption optimization on a system level is done, the fixed power consumption of monitoring and management electronics of each amplifier unit significantly affect the optimal point. If only the pump power consumption is taken into account, distributed Raman amplification is less energy efficient than only-EDFA based amplification due to the lower power conversion efficiency of the former. However, if the monitoring and management power consumption is accounted for, Raman amplification may be more energy efficient in some cases. This is due to the fact that the low-noise properties of distributed amplification allows longer spans while achieving the same OSNR and system length. Power savings using Raman amplification is possible if the monitoring and management power consumption is high, and the OSNR requirements are high.

We also use the model to compare PM-QPSK and PM-16QAM. We find that the higher spectral efficiency of 16QAM may lead to a lower energy consumption per bit, even though

the total power consumption is higher due to the higher OSNR requirement.

APPENDIX A
EDFA PUMP POWER FROM THE TWO-LEVEL MODEL

Here we compare the added-power model for EDFA pump power used in this work (described in Eq. (11)) with the pump power calculated with the two-level EDFA model described in [27]. The two-level model is valid assuming that the gain is not saturated by ASE. The guidelines provided in [27] states that this is true for gains less than 20 dB *or* input powers above $-$ 20 dBm. Assuming one pump and one signal wave, the two-level model has the solution

$$P_{\text{out}}^{p,s} = P_{\text{in}}^{p,s}\exp\left[\frac{P_{\text{in}}^{p,s} - P_{\text{out}}^{p,s}}{P_{\text{IS}}^{p,s}} + \right. \\ \left. + \frac{\lambda_{s,p}}{\lambda_{p,s}}\left(\frac{P_{\text{in}}^{s,p} - P_{\text{out}}^{s,p}}{P_{\text{IS}}^{s,p}}\right) - \alpha_{p,s}L_{\text{EDF}}\right], \tag{14}$$

where $P_{\text{out}}^{p,s}$ and $P_{\text{in}}^{p,s}$ are the pump or signal output and input power to the erbium-doped fiber (EDF). The absorption coefficient $\alpha_{p,s}$ and the intrinsic saturation power $P_{\text{IS}}^{p,s}$ are wavelength dependent EDF parameters whose definition can be found in [27], and L_{EDF} is the EDF length. This can be solved to yield

$$P_{\text{in}}^{p} - P_{\text{out}}^{p} = \frac{\lambda_s}{\lambda_p}\left(P_{\text{out}}^{s} - P_{\text{in}}^{s} + P_{\text{IS}}^{s}\left(\ln\frac{P_{\text{out}}^{s}}{P_{\text{in}}^{s}} + \alpha_s L_{\text{EDF}}\right)\right), \tag{15}$$

which, if $P_{\text{out}}^{p} << P_{\text{in}}^{p}$ and $P_{\text{IS}}^{s} << P_{\text{out}}^{s}$, is approximately equivalent to Eq. (10). The first condition states that the most of the pump power needs to be absorbed in the EDF, which is true for an EDFA with optimized EDF length. The second condition is that the intrinsic saturation power should be much smaller than the total signal output power. Based on EDF parameters in [28, Ch. 6], P_{IS}^{s} is less than 0.5 mW in the C-band, so this requirement is typically fulfilled for a filled WDM system.

In Fig. 12 the pump power found with the two models is plotted as a function of the gain for three different signal output powers. Pump and signal wavelengths are assumed to be 980 nm and 1550 nm respectively, and the EDF parameters in [28, Ch. 6] are used. In each point the EDF length is optimized for maximum energy conversion for the two-level model, and the energy conversion efficiency in the added-power model is chosen separately for each signal output power. This illustrates that the two models give similar results.

APPENDIX B
POWER CONSUMPTION OF A COOLED RAMAN PUMP LASER

We consider the total power consumption of the laser to be the sum of the power consumed by the laser and the power consumed by the thermoelectric cooler (TEC),

$$P_{\text{pump}}^{e} = P_{\text{laser}}^{e} + P_{\text{TEC}}^{e}, \tag{16}$$

where the laser power consumption is assumed to be proportional to the output optical power $P_{\text{laser}}^{e} = P_{\text{laser}}^{o}/\eta_{\text{laser}}$. The power consumption of the TEC is proportional to the heat removed from the laser chip, $P_{\text{TEC}}^{e} = Q_{\text{heat}}/\eta_{\text{TEC}}$, where η_{TEC} is known as the coefficient of performance (COP) [29]. The COP depends on the temperature difference between the hot and cold side of the TEC [29]. If the temperature difference is low it can reach above 100%, but for a 50 K difference not uncommon in telecommunication applications a typical value is below 20% [20].

The heat produced by the laser can be found by subtracting the optical output power from the power consumption.

$$P_{\text{TEC}}^{e} = \frac{1}{\eta_{\text{TEC}}}(P_{\text{laser}}^{e} - P_{\text{laser}}^{o}) = \frac{1}{\eta_{\text{TEC}}}\left(\frac{1}{\eta_{\text{laser}}} - 1\right)P_{\text{laser}}^{o}. \tag{17}$$

This leads to the the total power consumption

$$P_{\text{pump}}^{e} = \left(\frac{1}{\eta_{\text{laser}}} + \frac{1}{\eta_{\text{TEC}}\eta_{\text{laser}}} - \frac{1}{\eta_{\text{TEC}}}\right)P_{\text{laser}}^{o}, \tag{18}$$

which is proportional to the optical output power. For convenience we can write the power conversion efficiency in one factor so that $P_{\text{pump}}^{e} = P_{\text{laser}}^{o}/\eta$.

REFERENCES

[1] B. S. G. Pillai *et al.*, "End-to-end energy modeling and analysis of long-haul coherent transmission systems," *J. Lightw. Technol.*, vol. 32, no. 18, pp. 3093–3111, Sep. 2014.

[2] T. Frisch and S. Desbruslais, "Electrical power, a potential limit to cable capacity," in *Proc. SubOptic Conf.*, 2013, pp. 3–7.

[3] S. Desbruslais, "Maximizing the capacity of ultra-long haul submarine systems," in *Proc. 20th Eur. Conf. Netw. Opt. Commun.*, Jun. 2015, pp. 1–6.

[4] R. S. Tucker, "Green optical communications—Part I: Energy limitations in transport," *IEEE J. Sel. Topics Quantum Electron.*, vol. 17, no. 2, pp. 245–260, Mar. 2011.

[5] K. Hinton, P. Wang, P. Farrell, and B. Pilai, "Power consumption of erbium doped fibre amplified links," in *Proc. IEEE 4th Int. Conf. Big Data Cloud Comput.*, Dec. 2014, pp. 662–668.

[6] E. Desurvire, *Erbium-doped Fiber Amplifiers: Principles and Applications*. New York, NY, USA: Wiley, 1994.

[7] N. J. Doran and A. D. Ellis, "Minimising total energy requirements in amplified links by optimising amplifier spacing," *Opt. Express*, vol. 22, no. 16, pp. 19810–19817, Aug. 2014.

[8] A. Carena, V. Curri, G. Bosco, P. Poggiolini, and F. Forghieri, "Modeling of the impact of nonlinear propagation effects in uncompensated optical coherent transmission links," *J. Lightw. Technol.*, vol. 30, no. 10, pp. 1524–1539, May 2012.

[9] W. Van Heddeghem and F. Idzikowski, "Equipment power consumption in optical multilayer networks—Source data," Tech. Rep. IBCN-12-001-01, 2012. [Online]. Available: http://powerlib.intec.ugent.be/

[10] C. Headley and G. P. Agrawal, *Raman Amplification in Fiber Optical Communication Systems*. New York, NY, USA: Academic, 2005.

[11] V. Curri, A. Carena, P. Poggiolini, G. Bosco, and F. Forghieri, "Extension and validation of the GN model for non-linear interference to uncompensated links using Raman amplification," *Opt. Express*, vol. 21, no. 3, pp. 3308–3317, Feb. 2013.

[12] V. Curri and A. Carena, "Merit of Raman pumping in uniform and uncompensated links Supporting NyWDM transmission," *J. Lightw. Technol.*, vol. 34, no. 2, pp. 554–565, Jan. 2016.

[13] W. S. Pelouch, "Raman amplification: An enabling technology for long-haul coherent transmission systems," *J. Lightw. Technol.*, vol. 34, no. 1, pp. 6–19, Jan. 2016.

[14] L. Lundberg, P. Johannisson, E. Agrell, M. Karlsson, and P. A. Andrekson, "Power consumption of hybrid EDFA/Raman amplified systems," in *Proc. Eur. Conf. Opt. Commun.*, Sep. 2015, Art. no. P.5.15.

[15] P. Wang, K. Hinton, P. M. Farrell, and B. S. G. Pillai, "On EDFA and Raman fiber amplifier energy efficiency," in *Proc. IEEE Int. Conf. Data Sci. Data Intensive Syst.*, Dec. 2015, pp. 268–275.

[16] "Finisar Raman amplifier module," Sep. 16, 2016. [Online]. Available: https://www.finisar.com/optical-amplifiers/foa-r9000de-rbw2c-aa002
[17] E. Pincemin *et al.*, "Raman gain efficiencies of modern terrestrial transmission fibers in S-, C- and L-band," in *Proc. Nonlinear Guid. Waves Appl. Conf.*, 2002, Art. no. NLTuC2.
[18] P. Johannisson and E. Agrell, "Modeling of nonlinear signal distortion in fiber-optic networks," *J. Lightw. Technol.*, vol. 32, no. 23, pp. 4544–4552, Dec. 2014.
[19] J. Yoshida *et al.*, "2.8 FITs of field reliability of 1480nm/14xx-nm pump lasers," in *Proc. Opt. Fiber Commun. Conf.*, 2015, Art. no. W2A.2.
[20] L. A. Johnson, *Application note: Controlling Temperatures of Diode Lasers and Detectors Thermoelectrically*, Newport Corporation, Irvine, CA, USA, Nov. 7, 2016. [Online]. Available: https://www.newport.com/medias/sys_master/images/images/hcc/hc7/8797049389086/AN01-Controlling-Temperatures-of-Laser-Diodes-Thermoelectrically.pdf
[21] W. Van Heddeghem, F. Idzikowski, W. Vereecken, D. Colle, M. Pickavet, and P. Demeester, "Power consumption modeling in optical multilayer networks," *Photon. Netw. Commun.*, vol. 24, no. 2, pp. 86–102, 2012.
[22] V. Curri and A. Carena, "HFA optimization for NyWDM tranmission," in *Proc. Opt. Fiber Commun. Conf.*, 2015, Art. no. W4E.4.
[23] J. G. Proakis and M. Salehi, *Digital Communications*, 5th ed. New York, NY, USA: McGraw-Hill, 2008.
[24] K. Cushon, P. Larsson-Edefors, and P. Andrekson, "Low-power 400-Gbps soft-decision LDPC FEC for optical transport networks," *J. Lightw. Technol.*, vol. 34, no. 18, pp. 4304–4311, Sep. 2016.
[25] E. Agrell, A. Alvarado, G. Durisi, and M. Karlsson, "Capacity of a nonlinear optical channel with finite memory," *J. Lightw. Technol.*, vol. 32, no. 16, pp. 2862–2876, Aug. 2014.
[26] G. Bosco, P. Poggiolini, A. Carena, V. Curri, and F. Forghieri, "Analytical results on channel capacity in uncompensated optical links with coherent detection," *Opt. Express*, vol. 19, no. 26, pp. B440–B451, Dec. 2011.
[27] A. A. M. Saleh, R. M. Jopson, J. D. Evankow, and J. Aspell, "Modeling of gain in erbium-doped fiber amplifiers," *IEEE Photon. Technol. Lett.*, vol. 2, no. 10, pp. 714–717, Oct. 1990.
[28] P. C. Becker, N. A. Olsson, and J. R. Simpson, *Erbium-Doped Fiber Amplifiers: Fundamentals and Technology*. San Diego, CA, USA: Academic, 1999.
[29] D. Enescu and E. O. Virjoghe, "A review on thermoelectric cooling parameters and performance," *Renew. Sustain. Energy Rev.*, vol. 38, pp. 903–916, 2014.

Lars Lundberg received the M.Sc. degree in engineering physics from Chalmers University of Technology, Gothenburg, Sweden, in 2013. In 2014, he joined the Photonics Laboratory, Department of Microtechnology and Nanoscience, Chalmers University of Technology, where he is currently working toward the Ph.D. degree. His research interests are mainly focused on energy consumption of fiber optical communication systems

Peter A. Andrekson (F'06) received the Ph.D. degree from Chalmers University of Technology, Gothenburg, Sweden, in 1988. After about three years with AT&T Bell Laboratories, Murray Hill, NJ, USA, during 1989–1992, he returned to Chalmers University of Technology, where he is currently a Full Professor at the Department of Microtechnology and Nanoscience. He was the Director of Research at Cenix Inc., Allentown, PA, USA, during 2000–2003 and with the newly established Center for Optical Technologies at Lehigh University, Bethlehem, PA, during 2003–2004. He is the co-Founder of the optical test and measurement company Picosolve Inc., which is now part of EXFO. He has authored about 450 scientific publications and conference papers in the area of optical communications, among which more than 90 were invited papers at leading international conferences and journals, including three tutorials at the Optical Fiber Communication Conference (OFC) in 2004, 2011, and 2014. His research interests include nearly all aspects of fiber communications such as optical amplifiers, nonlinear pulse propagation, all-optical functionalities, and very high capacity transmission.

Dr. Andrekson is a Fellow of the Optical Society of America. He was an elected member of the Board of Governors for the IEEE Photonics Society (2011–2013) and is or has served on several technical program committees, including OFC and European Conference of Optical Communication, and as an International Project and Candidate Evaluator, and has also twice served as an expert for the evaluation of the Nobel Prize in Physics. He was an Associate Editor for IEEE PHOTONICS TECHNOLOGY LETTERS during 2003–2007. In 1993, he was awarded a price from the Swedish government research committee for outstanding work performed by young scientists, and in 2000, he received the Telenor Nordic Research Award for his contribution to optical technologies.

Magnus Karlsson (SM'13) received the Ph.D. degree from Chalmers University of Technology, Gothenburg, Sweden, in 1994. Since 1995, he has been with the Photonics Laboratory at Chalmers University of Technology, first as an Assistant Professor and since 2003 as a professor in photonics. He has authored or coauthored around 300 scientific journal and conference contributions in the areas of nonlinear optics and fiber-optic transmission. He co-founded the Chalmers Fiber-Optic Communication Research Center, FORCE, in 2010.

Dr. Karlsson serves in the technical program committees for the Optical Fiber Communication Conference and the European Conference of Optical Communication (ECOC), and is also active in the committees for the IEEE Global Communications Conference and the IEEE International Conference on Communications. He is a Deputy Editor for *Optics Express* and has served as a Guest Editor for the JOURNAL OF LIGHTWAVE TECHNOLOGY. He contributed to the 100-GET and EO-Net projects that were both awarded the CELTIC Excellence Award. He supervised students receiving the Best Paper Awards at GlobeCom 2011 and ECOC 2012. He is a Fellow of the Optical Society of America.